IEEE Access
Multidisciplinary | Rapid Review | Open Access Journal

Received February 12, 2019, accepted February 24, 2019, date of publication March 6, 2019, date of current version March 25, 2019.

Digital Object Identifier 10.1109/ACCESS.2019.2903146

Integral Imaging With Full Parallax Based on Mini LED Display Unit

WEI WU[1,2], (Student Member, IEEE), SHIGANG WANG[1], CHENG ZHONG[3], MEILAN PIAO[1], AND YAN ZHAO[1], (Member, IEEE)

[1]School of Communication Engineering, Jilin University, Changchun 130012, China
[2]School of Computer Science and Engineering, Changchun University of Technology, Changchun 130012, China
[3]School of Public Administration, Changchun University of Technology, Changchun 130012, China

Corresponding authors: Wei Wu (114188246@qq.com) and Shigang Wang (wangshigang@vip.sina.com)

This work was supported in part by the National Key Research and Development Program of China under Grant 2017YFB0404800, in part by the National Natural Science Foundation of China under Grant 61631009, in part by the National Natural Science Foundation of China under Grant 61705076, and in part by the Fundamental Research Funds for the Central Universities under Grant 2017TD-19.

ABSTRACT Integral imaging has been considered as the most applicable technology of true 3D display in the near future. In this paper, we propose the method to achieve full parallax and large-screen integral imaging display based on mini LED. Compared to the existing integral imaging systems based on the LED, the proposed method can present both horizontal and vertical parallaxes. We explore the optical parameter matching method between mini LED display unit and lenslet unit and design three different shapes of lenslet arrays. The imaging performance of lenslet arrays of circular-shape, square-shape, and hexagonal-shape is analyzed. The method of window interception is proposed to generate elemental images for the lenslet arrays with different apertures and arranging structures. The experimental results show that the true 3D display with full parallax and screen scalability has been realized using the proposed method and the display effect of lenslet array with hexagonal-shape is the best according to the evaluation of both subjective and objective merits.

INDEX TERMS Elemental image, integral imaging, mini LED, lenslet array.

I. INTRODUCTION

Integral imaging is a type of true three-dimensional (3D) image display technology that reconstructs the stereoscopic optical model of the original scenes through light superposition, and recovers the relative depth information of the real scenes lost in the projection process. Viewers can view 3D images with physical depth-of-focus through only their naked eyes. The advantages of integral imaging include real image colors, complete parallax, multiple viewing angles, simultaneous viewing by multiple viewers, and real-time interaction [1]. Therefore the integral imaging may have a broad application prospect in entertainment, medicine, military affairs, production, life, and other fields.

The research on integral imaging focuses mainly on real-time handling of 3D information and improvement of viewing parameters. Kim *et al.* [2] developed a real-time capturing and displaying 3D autostereoscopic system. Kim *et al.* [3] solved the pseudoscopic problem in real-time by using a conversion algorithm. Furthermore, Kim *et al.* [4] proposed a method that enhances the processing speed in real-time 3D displays. Many studies have also been conducted on improving the viewing resolution [5]–[9], widening the viewing angle [10]–[14], and enhancing the depth of 3D image [15]–[17].

Notably, the aforementioned studies are mainly based on the display device of a liquid-crystal display (LCD), projector and LED. When implementing a large-screen 3D display, multiple display devices must be combined. It is difficult to combine multiple LCDs without a boarder [18]. The projector array must be calibrated; its display process is complex, and is thus not suitable for moving [19]. Large screen display of LED is often built by multiple LED display units (LDU). Inspired by this idea we propose to optically match LDU and lenslet unit (LU) to build the integral imaging display unit (IIDU). Consequently multiple IIDUs can be combined to achieve any size of large-screen integral imaging display as needed. Yang *et al* proposed a large-size horizontal light-filed

The associate editor coordinating the review of this manuscript and approving it for publication was Yuming Fang.

display based on the LED which can only present the horizontal parallax of 3D image [20]. However, the vertical parallax cannot be omitted for a true 3D display. The optical matching method we proposed can present both horizontal and vertical parallaxes and provides the theory for implementing large-sized, full parallax, high-resolution display of integral imaging in engineering.

The rest of the paper is organized as follows. The integral imaging system based on mini LED is introduced in Section 2. In Section 3, we explain the optical parameter matching and optimization. In Section 4, we introduce the Elemental image array generation based on window interception. Section 5 provides the experimental results. Finally, a brief summary is given in Section 6.

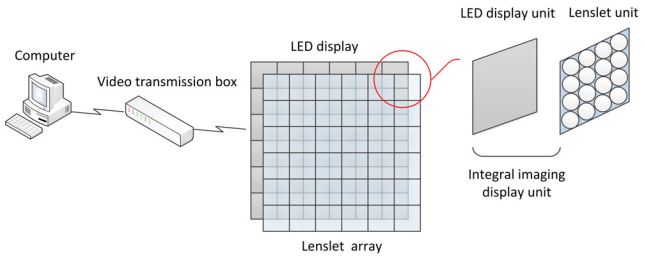

FIGURE 1. Integral imaging based on a mini LED.

II. INTEGRAL IMAGING SYSTEM BASED ON MINI LED

The integral imaging system based on mini LED is composed of a computer, video transmission box, mini LED, and lenslet array, as shown in Fig. 1. The video signal is transformed to a network signal via a video transmission box, which is controlled by the computer and sent to the LED display. The 3D image is reconstructed around the central depth plane, at which the lights emitted from the LED are refracted by the lenslet array and converged.

The integral imaging display unit (IIDU) is composed of the LED display unit (LDU) and lenslet unit (LU), which can be combined to achieve various display modes such as flat, arc, and scalene, as needed.

The structure of the mini LED display is shown in Fig. 2(a). Each LDU is composed of 96×96 LED pixels, and each pixel includes red, green, and blue LEDs with an integrated, three-in-one packaging structure that significantly reduces the pixel size, thus resulting in a seamlessly combined LDU.

The lenslet array is optically designed according to the LDU, as shown in Fig. 2(b). There are M $\times$ N lenslet units in the lenslet array and each lenslet unit has m $\times$ n lenslets. The main parameters of the LU are the quantity, diameter d, pitch p, focal length, shape, and arrangement of the lenslet. These parameters are closely related to the resolution, viewing angle, and depth of the 3D image. The reduction of the diameter can increase the quantity of the lenslet per unit area, and the resolution of the 3D image improves accordingly. In addition, by increasing the focal length, the depth of the 3D image can be increased.

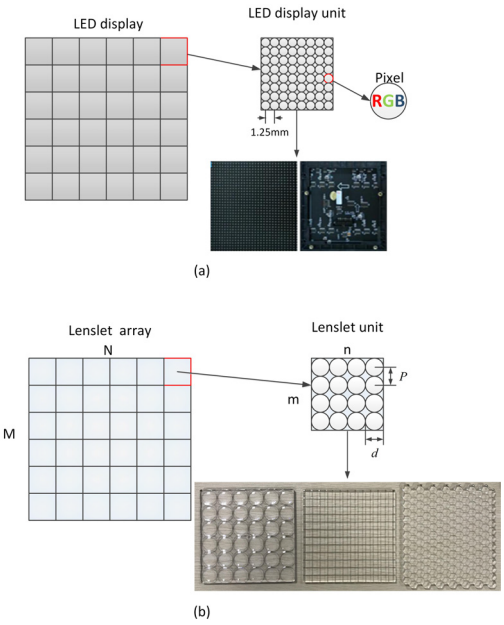

FIGURE 2. Model of (a) LED display unit and (b) lenslet unit.

III. OPTICAL PARAMETER MATCHING AND OPTIMIZATION

The optical design of the lenslet can determine the parameters of the radius of curvature R, diameter of the photoresist D, height of the spherical crown h, and height of the basement H according to the diameter d and focal length f of the lenslet. The optical design of the LU determines the quantity of lenslet in the LU and the thickness of the photoresist according to the shape, pitch, and arrangement of the lenslet.

Circular, square, and hexagonal lenslet arrays with different apertures are optical designed. The square lenslet array has a higher filling factor than the circular lenslet array, while the hexagonal lenslet array further increases the sampling rate and improves resolution of the 3D image per unit area. As the hexagonal lenslet array cannot be completely divided by the square shape, the hexagonal lenslet is completely reserved on the jagged edge of a hexagonal LU. In this manner, the segmented hexagonal lenslet array can be completely restored by combining multiple hexagonal LUs.

A. OPTICAL PARAMETERS OF THE LENSLET

Fig. 3 shows the optical design of the circular, square, and hexagonal lenslets. The number of pixels in an LDU is in multiples of 8, i.e. usually 64×64 or 96×96; thus, the diameter of the lenslet is obtained by

$$d = 8ks \tag{1}$$

where, s is the pixel size of the LED. The diameter of a lenslet is smaller than the size of an LDU; thus, $k = 1, 2, \ldots 8$ if using a 64×64 LDU or $k = 1, 2, \ldots 12$ if using a 96×96 LDU. The focal length of the lenslet can be set according to

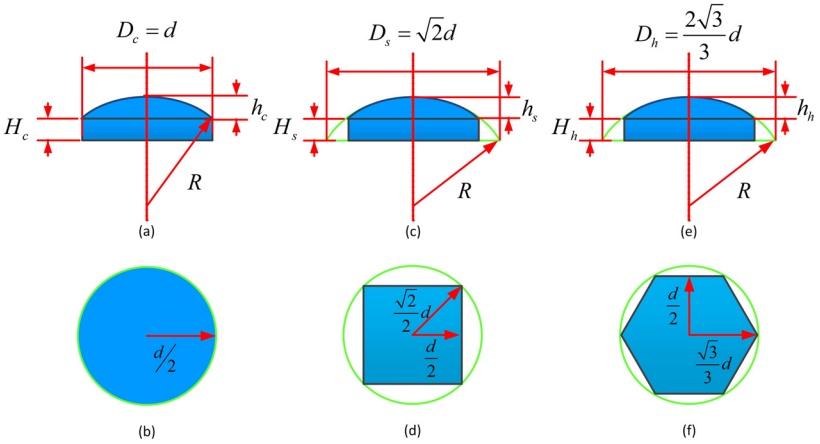

FIGURE 3. Optical parameters of lenslet. The profile and top view of (a) (b) circular, (c) (d) square, and (e) (f) hexagonal lenslets.

the central depth plane as

$$f = \frac{L}{Nn - 1} \tag{2}$$

where, L is the distance between the lenslet array and central depth plane, N and n are the number of LUs and the number of lenslets in an LU, respectively. The radius of curvature is

$$R = f(n_r - 1) \tag{3}$$

where, n_r is the refractive index. Then, the diameter of the photoresist and the height of the spherical crown are given respectively by

$$D_c = d \quad h_c = R - \sqrt{R^2 - \frac{d^2}{4}} \tag{4}$$

for the circular lenslet,

$$D_s = \sqrt{2}d \quad h_s = R - \sqrt{R^2 - (\frac{\sqrt{2}}{2}d)^2} \tag{5}$$

for the square lenslet, and

$$D_h = \frac{2\sqrt{3}}{3}d \quad h_h = R - \sqrt{R^2 - (\frac{\sqrt{3}}{3}d)^2} \tag{6}$$

for the hexagonal lenslet

The height of the basement H_c for the circular lenslet can be set between 3-5 mm and those for the square (H_s) and hexagon (H_h) are respectively given by

$$H_s = \sqrt{R^2 - (\frac{d}{2})^2} - \sqrt{R^2 - (\frac{\sqrt{2}}{2}d)^2} \tag{7}$$

$$H_h = \sqrt{R^2 - (\frac{d}{2})^2} - \sqrt{R^2 - (\frac{\sqrt{3}}{3}d)^2} \tag{8}$$

B. OPTICAL PARAMETERS OF THE LU

The optical templates of the circular, square, and hexagonal LUs designed based on the LDU are shown in Fig. 4. The lenslet is closely packed with lens pitch $p = d$, where d is the diameter of the inscribed circle. The number of pixels of the LDU is calculated by $P_h \times P_v$, and the numbers $m_c \times n_c$, $m_s \times n_s$ of the circular and square lenslets in the LUs are calculated by

$$m_c = m_s = \frac{sP_h}{d} \quad n_c = n_s = \frac{sP_v}{d}, \tag{9}$$

while the number $m_h \times n_h$ of the hexagonal lenslet is calculated by

$$m_h = \frac{sP_h}{d} \quad n_h = \frac{2\sqrt{3}}{3}\frac{sP_v}{d} \tag{10}$$

The thickness of the photoresist of the three lenslets are obtained by

$$t_c = \frac{h_c}{6}(3 + 4\frac{h_c^2}{D_c^2}), \tag{11}$$

$$t_s = \frac{\pi h_s^2(R - \frac{h_s}{3})}{P^2}, \tag{12}$$

$$t_h = \frac{2\pi h_h^2(R - \frac{h_h}{3})}{\sqrt{3}P^2}. \tag{13}$$

where, subscripts c, s, and h represent the circular, square, and hexagonal lenslets, respectively.

Owing to the square shape of the LDU, the optical template of the LU, which is designed based on the LDU, should also be square. However, an integral number of hexagonal lenslets cannot be contained in a square; therefore, we reserve the whole lenslet on the edge of the optical template of the LU and completely restore the segmented hexagonal lenslet array.

C. IMAGING PERFORMANCE ANALYSIS OF THE LU

In the 3D reconstruction, the rays pass through the lenslet array and form the 3D image around the central depth plane.

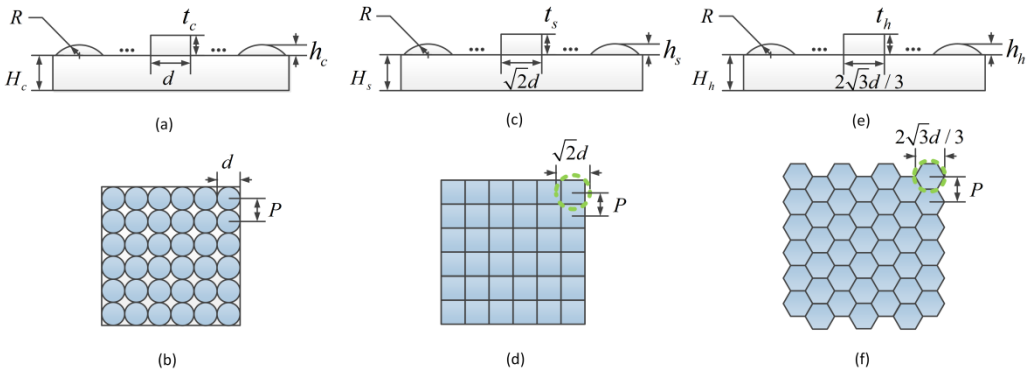

FIGURE 4. Optical template of LU. The profile and top view of (a) (b) circular, (c) (d) square, and (e) (f) hexagonal lenslets.

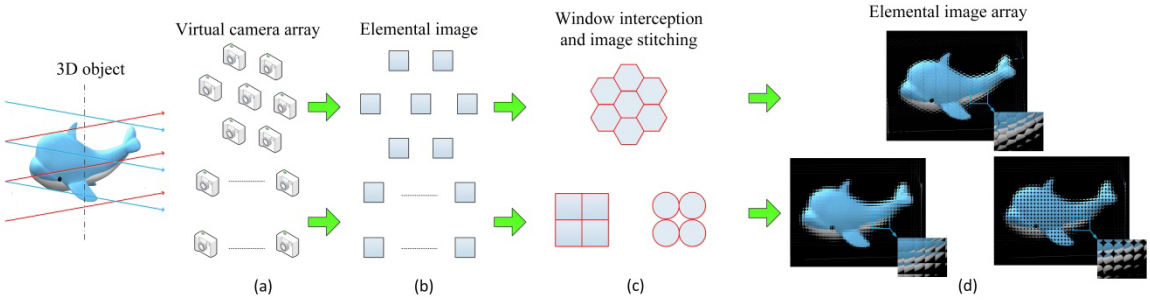

FIGURE 5. Process of elemental image array generation using window interception. (a) Virtual camera array. (b) Elemental image. (c) Window interception and image stitching. (d) Elemental image array.

A 3D image consists of many 3D image points with different shapes and depths. The sampling rate determines the number of 3D image points and is directly proportional to the 3D image resolution. The filling factor determines the transmission efficiency of the optical information. Therefore, the product of the filling factor and sampling rate of the LU are the main factors that affect the 3D images. The filling factor is a measure of the total optical information of a lenslet array. It is defined as the ratio of the active light area to the total light area [21], and it does not vary with the shape and size of the lenslet array. The filling factor is given by

$$\eta = \frac{S_{active}}{S_{total}}. \tag{14}$$

In Fig. 4(b), (d), and (f), S_{active} is the active imaging area (the area of light that can be imaged through a lens) and S_{total} is the area of the whole lenslet array. Eq. (14) shows that in the same area, smaller gaps between the lenslets lead to a larger value of S_{active}. Thus, the more the amount of optical information obtained by the lenslet array is, the better the imaging effect is. By simple geometrical computation, we can obtain the filling factors as 0.785 for (b), 1 for (d), and 1 for (f), respectively.

The sampling rate of the lenslet array is defined as

$$\beta = \frac{S_{active}}{S_{lens}} = \frac{\eta S_{total}}{S_{lens}}. \tag{15}$$

The unit employed in Eq.(15) is the number of sampling points per unit area. The sampling rate is related to the shape, size, and arrangement of the lenslet. For example, in the area of $6d \times 6d$ (as shown in Fig. 4), the sampling rates for Figs. 4(b), (d), and (f) are 36, 36, and 41.4, respectively.

Therefore, for a circular lenslet array, a gap exists between the lenslets, which leads to 21.5% of the optical information loss and degrades the 3D image quality. Given the same inscribed circle aperture d and lens pitch p, the hexagonal lenslet array, which has both higher filling factor and sampling rate than the square and circular arrays, can reconstruct a better 3D image [22]–[23].

IV. ELEMENTAL IMAGE ARRAY GENERATION BASED ON WINDOW INTERCEPTION

To generate elemental images used for different apertures of lenslet arrays, we present a method that can generate an elemental image array through window interception. The sampling model is established according to the structure of the lenslet array, and the elemental images of the 3D object, which correspond to each virtual lens, are calculated according to the optical parameters of the display platform. And the window interception is used to generate the elemental image array. The elemental image array with any aperture and any arranging structure can be generated by changing the sampling points and window function. The principle of this method is shown in Fig. 5.

TABLE 1. System parameters.

Computer	Intel(R) Core(TM) i7-7700 CPU @ 4.2 GHZ 16 GB RAM			
Video transmission box	1 Gbps			
LED	Resolution of LED	384 × 384	Size of LED	480 × 480 mm
	Resolution of LDU	96 × 96	Size of LDU	120 × 120 mm
	Pixel size	1.25 mm	Color space	2500-10000 k
Lenslet array	Size of LU (mm)	Number of lenslet in LU	Diameter (mm)	Focal length (mm)
Circular	120 ×120	6 × 6	20	60
Square	120 × 120	12 × 12	10	60
Hexagonal	120 × 120	12 × 13.8	10	60

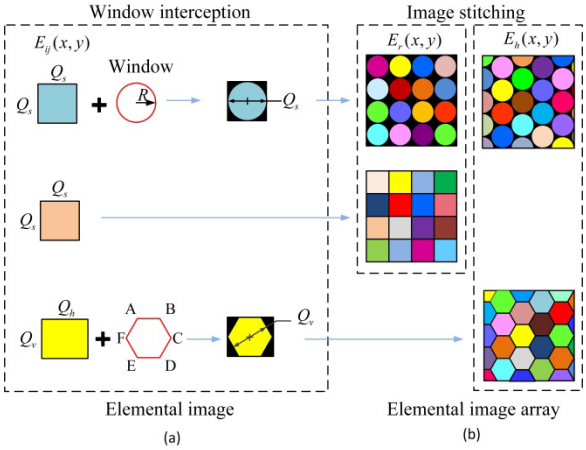

FIGURE 6. (a) Window interception and (b) image stitching.

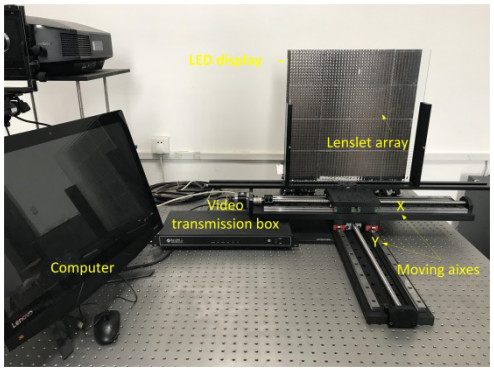

FIGURE 7. Proposed integral imaging system based on a mini LED.

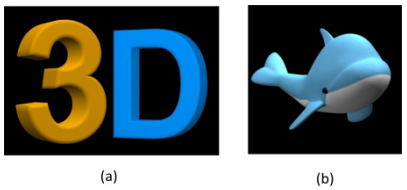

FIGURE 8. Test objects. (a) Alphabetical patterns and (b) Dolphin.

The elemental image array used for the square lenslet array is generated by directly stitching the elemental image in the rectangular sampling structure. In contrast, the elemental image array used for the circular or hexagonal lenslet array is generated by stitching the elemental image, which is cropped using a circular or hexagonal window function, in a rectangular or honeycomb sampling structure.

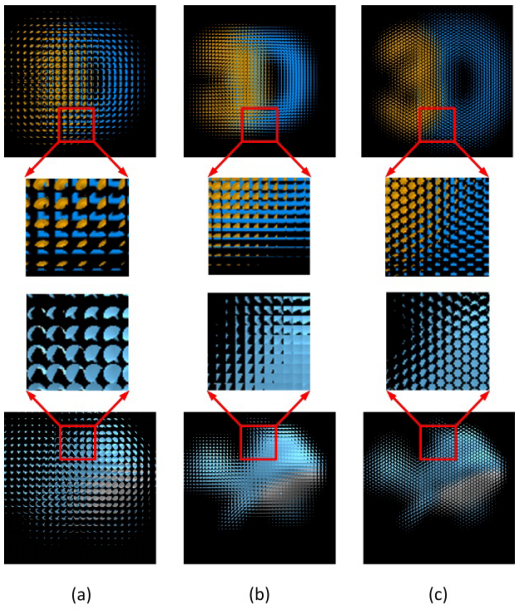

FIGURE 9. Elemental image arrays. (a) Circular. (b) Square. (c) Hexagonal.

As shown in Fig. 6(a), if the resolution of the elemental image is $Q_s \times Q_s$ or $Q_h \times Q_v$, the upper left corner is considered as the origin of the coordinates and the centre of the window function is same as the centre of the elemental image. Then, the radius of the circular window function is $R = Q_s/2$, and the vertex coordinates of the hexagonal window function in each elemental image is given by

$$\begin{aligned} &\mathrm{A}(0,\frac{1}{4}Q_h) \quad \mathrm{B}(0,\frac{3}{4}Q_h) \\ &\mathrm{C}(\frac{1}{2}Q_v, Q_h) \quad \mathrm{D}(Q_v, \frac{3}{4}Q_h) \\ &\mathrm{E}(Q_v, \frac{1}{4}Q_h) \quad \mathrm{F}(\frac{1}{2}Q_v, 0) \end{aligned} \tag{16}$$

As shown in Fig. 6(b), if the lenslet array consists of $m \times n$ lenslets, then the stitching coordinates of the (i,j) elemental image $E_{ij}(x, y)$ in the rectangular sampling elemental image array $E_r(x, y)$ becomes

$$\begin{aligned} &E_{ij}(x, y) = E_r(x + Q_s(i-1), y + Q_s(j-1)) \\ &\quad i = 1, 2, \ldots m; \quad j = 1, 2 \ldots n; \; x, y = 1, 2 \ldots Q_s \end{aligned} \tag{17}$$

and the resolution of $E_r(x, y)$ is $mQ_s \times nQ_s$. The stitching coordinate of the (i,j) elemental image $E_{ij}(x, y)$ in the

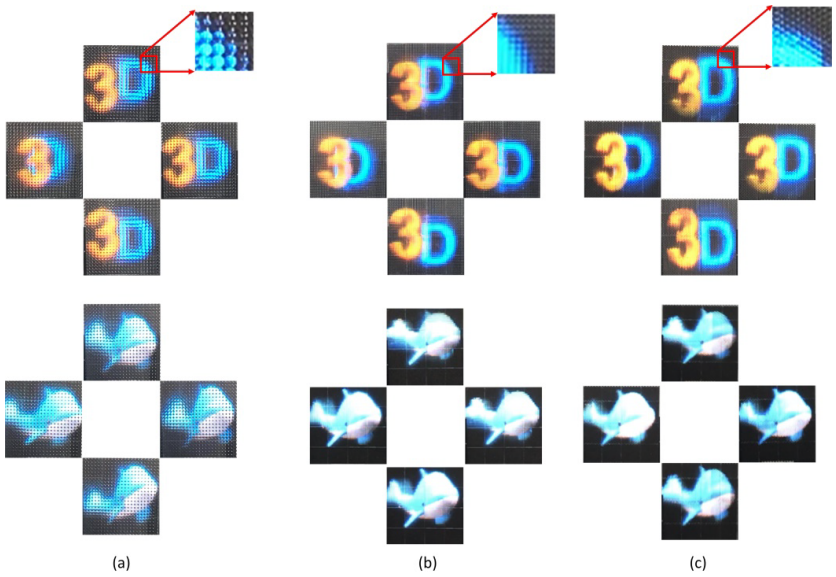

FIGURE 10. 3D images reconstructed by (a) circular, (b) square, and (c) hexagonal lenslet arrays. (see Visualization 1: 3D display with full parallax).

hexagonal sampling elemental image array $E_h(x, y)$ can be expressed as

$$E_{ij}(x,y) = \begin{cases} E_h(x + Q_v(i-1), \quad y + \frac{3}{4}Q_h(j-1)) \\ \quad i = 1, 2 \ldots m; \quad j = 1, 3, 5 \ldots n; \\ \quad x = 1, 2 \ldots Q_v; \quad y = 1, 2 \ldots Q_h \\ E_h(x + \frac{1}{2}Q_v + Q_v(i-1) \quad y + \frac{3}{4}Q_h + \frac{3}{4}Q_h(j-2)) \\ \quad i = 1, 2 \ldots m; \quad j = 2, 4, 6 \ldots n; \\ \quad x = 1, 2 \ldots Q_v; \quad y = 1, 2 \ldots Q_h \end{cases} \tag{18}$$

and the resolution of $E_h(x, y)$ is

$$(m \times Q_v + \frac{1}{2} \times Q_v) \times (Q_h + (n-1) \times \frac{3}{4}Q_h).$$

V. EXPERIMENTS

The proposed integral imaging system based on a mini LED is shown in Fig. 7. It is composed of a computer, video transmission box, mini LED, and lenslet array. The computer is used to control the display content, and the LED display and lenslet array are used for the display. The LED display is composed of 4×4 LED modules, and each module consists of 96×96 pixels. The designed lenslet array is composed of 4×4 LUs, and each LU is of the same size as the LDU. The gap between the lenslet array and LED display is adjusted by moving Y axis of the display platform; each elemental image and each lens are precisely aligned by moving X axis of the display platform. The details of the parameters are listed in Table 1.

The test objects comprise a *Dolphin* and two alphabetical patterns. The '3' and 'D' are longitudinally located at $z = 30$cm and $z = -30$cm, and the *Dolphin* is located at $z = 0$, as shown in Fig. 8. The resolution of the circular, square, and hexagonal elemental image array is 384×384, which are generated through window interception, as shown in Fig. 9.

The elemental image arrays are displayed on the proposed LED display platform, and the 3D image is captured from different perspectives as shown in Fig. 10. It shows that the proposed integral imaging based on the mini LED can actually reconstruct the 3D image with bright colours, realistic effects, and continuous horizontal and vertical parallaxes. The 3D image generated by the hexagonal lenslet array is clearer than that generated by the square array, which has the same diameter as that of the inscribed circle and lens pitch. This is due to the fact that the hexagonal lenslet array has higher sampling rate, which leads to higher resolution. The diameter of the inscribed circle of the circular lenslet array is the largest; thus, there are more subimages of the 3D image.

VI. CONCLUSIONS

We present the integral imaging system with full parallax based on mini LED, propose the methods of optical parameter matching and optimization, and design three shapes of lenslet arrays. It is a novel method to realize a large-screen true 3D display by seamlessly combining IIDUs. The IIDU is composed of an LDU and LU, and can achieve various display modes such as flat, arc, and scalene. Circular, square, and hexagonal LUs are optical matched with the LDU. Experimental results verified that the proposed method can actually reconstruct true 3D image with continuous horizontal and vertical parallaxes. Given the same inscribed circular aperture and lenslet pitch, the resolution of the 3D image generated by the hexagonal lenslet array is better than by the square lenslet array. The pixel pitch of mini LED is 0.5mm-1.5mm which can be reduced to 0.001 for micro LED in the near future, and the proposed optical matching method provides

the theory for implementing large-sized, full parallax, high-resolution display of integral imaging.

REFERENCES

[1] B. Javidi, F. Okano, and J.-Y. Son, *Three-dimensional Imaging, Visualization, and Display*. New York, NY, USA: Springer Science+Business Media, 2009.
[2] J. Kim, J.-H. Jung, Y. Jeong, K. Hong, and B. Lee, "Real-time integral imaging system for light field microscopy," *Opt. Express*, vol. 22, no. 9, pp. 10210–10220, May 2014.
[3] J. Kim, J.-H. Jung, C. Jang, and B. Lee, "Real-time capturing and 3D visualization method based on integral imaging," *Opt. Express*, vol. 21, no. 16, pp. 18742–18753, Aug. 2013.
[4] D.-H. Kim *et al.*, "Real-time 3D display system based on computer-generated integral imaging technique using enhanced ISPP for hexagonal lens array," *Appl. Opt.*, vol. 52, no. 34, pp. 8411–8418, Dec. 2013.
[5] C. Yang, J. Wang, A. Stern, S. Gao, V. Gurev, and B. Javidi, "Three-dimensional super resolution reconstruction by integral imaging," *J. Display Technol.*, vol. 11, no. 11, pp. 947–952, Nov. 2015.
[6] J.-Y. Jang, D. Shin, B.-G. Lee, and E.-S. Kim, "Multi-projection integral imaging by use of a convex mirror array," *Opt. Lett.*, vol. 39, no. 10, pp. 2853–2856, May 2014.
[7] X. Li, L. Li, and Q.-H. Wang, "Wavelet-based iterative perfect reconstruction in computational integral imaging ," *J. Opt. Soc. Amer. A, Opt., Image Sci., Vis.*, vol. 35, no. 7, pp. 1212–1220, Jul. 2018.
[8] J.-S. Jang, Y.-S. Oh, and B. Javidi, "Spatiotemporally multiplexed integral imaging projector for large-scale high-resolution three-dimensional display," *Opt. Express*, vol. 12, no. 4, pp. 557–563, Feb. 2004.
[9] H. Liao, M. Iwahara, N. Hata, and T. Dohi, "High-quality integral videography using a multiprojector," *Opt. Express*, vol. 12, no. 6, pp. 1067–1076, Mar. 2004.
[10] H. Choi, S.-W. Min, S. Jung, J.-H. Park, and B. Lee, "Multiple-viewing-zone integral imaging using a dynamic barrier array for three-dimensional displays," *Opt. Express*, vol. 11, no. 8, pp. 927–932, Apr. 2003.
[11] B. Lee, S. Jung, and J.-H. Park, "Viewing-angle-enhanced integral imaging by lens switching," *Opt. Lett.*, vol. 27, no. 10, pp. 818–820, May 2002.
[12] X. Yu *et al.*, "Large viewing angle three-dimensional display with smooth motion parallax and accurate depth cues," *Opt. Express*, vol. 23, no. 20, pp. 25950–25958, Oct. 2015.
[13] S. W. Min, S. Jung, J. H. Park, and B. Lee, "Study for wide-viewing integral photography using an aspheric Fresnel-lens array," *Opt. Eng.*, vol. 41, no. 10, pp. 2572–2576, Oct. 2002.
[14] S. Jung, J.-H. Park, H. Choi, and B. Lee, "Wide-viewing integral three-dimensional imaging by use of orthogonal polarization switching," *Appl. Opt.*, vol. 42, no. 14, pp. 2513–2520, May 2003.
[15] H. Choi, Y. Kim, J.-H. Park, J. Kim, S.-W. Cho, and B. Lee, "Layered-panel integral imaging without the translucent problem," *Opt. Express*, vol. 13, no. 15, pp. 5769–5776, Jul. 2005.
[16] H. Liao, M. Iwahara, Y. Katayama, N. Hata, and T. Dohi, "Three-dimensional display with a long viewing distance by use of integral photography," *Opt. Lett.*, vol. 30, no. 6, pp. 613–615, Mar. 2005.
[17] H. Liao, T. Dohi, and K. Nomura, "Autostereoscopic 3D display with long visualization depth using referential viewing area-based integral photography," *IEEE Trans. Vis. Comput. Graphics*, vol. 17, no. 11, pp. 1690–1701, Nov. 2011.
[18] N. Okaichi, M. Miura, J. Arai, M. Kawakita, and T. Mishina, "Integral 3D display using multiple LCD panels and multi-image combining optical system," *Opt. Express*, vol. 25, no. 3, pp. 2805–2817, Feb. 2017.
[19] P. Wang *et al.*, "A large depth of field frontal multi-projection three-dimensional display with uniform light field distribution," *Opt. Commun.*, vol. 354, pp. 321–329, Nov. 2015.
[20] L. Yang *et al.*, "Demonstration of a large-size horizontal light-field display based on the LED panel and the micro-pinhole unit array," *Opt. Commun.*, vol. 414, pp. 140–145, May 2018.
[21] J.-S. Jang and B. Javidi, "Improvement of viewing angle in integral imaging by use of moving lenslet arrays with low fill factor," *Appl. Opt.*, vol. 42, no. 11, pp. 1996–2002, Apr. 2003.
[22] W. Wu, S. Wang, M. Piao, Y. Zhao, and J. Wei, "Performance metric and objective evaluation for displayed 3D images generated by different lenslet arrays," *Opt. Commun.*, vol. 426, pp. 635–641, Nov. 2018.
[23] N. Chen, J. Yeom, J.-H. Jung, J.-H. Park, and B. Lee, "Resolution comparison between integral-imaging-based hologram synthesis methods using rectangular and hexagonal lens arrays," *Opt. Express*, vol. 19, no. 27, pp. 26917–26927, Dec. 2011.

WEI WU (S'18) received the M.S. degree in signal and information processing from the Changchun University of Technology, in 2009. She is currently pursuing the Ph.D. degree with the School of Communication Engineering, Jilin University, and a Teacher with the School of Computer Science and Engineering, Changchun University of Technology. Her research interests include optical information processing, 3D display, and image processing.

SHIGANG WANG received the Ph.D. degree in communication and information systems from Jilin University, China, in 2001, where he is currently a Professor. He is the Director of the China Society of Image and Graphics and the Vice Chair of Jilin Province Society of Image and Graphics. He has authored or co-authored many papers. He holds patents in recent years. He was a recipient of many awards, which include the China Institute of Communications Science and Technology Prize and the Jilin Province Science and Technology Progress Award and Technology Invention Award. His research interests include true-3D display and 3D image processing, and digital vision.

CHENG ZHONG received the B.S. degree in computer science and technology and the M.S. degree in computer technology from the Changchun University of Technology, Changchun, China, in 2001 and 2009, respectively, where he is currently an Associate Professor. His research interests include computer vision, machine learning, 3D display, and image processing.

MEILAN PIAO received the M.S. and Ph.D. degrees from Chungbuk National University, South Korea, in 2009 and 2014, respectively. Subsequently, she held one year postdoctoral position at the Department of Information Communication Engineering, Chungbuk National University. She is currently an Assistant Professor with the Department of Communication Engineering, Jilin University, China. Her research interests include optical information processing, computer-generated hologram, and 3D display.

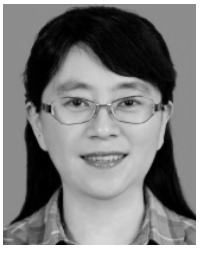

YAN ZHAO (M'10) received the B.S. degree in communication engineering from the Changchun Institute of Posts and Telecommunications, in 1993, the M.S. degree in communication and electronic from the Jilin University of Technology, in 1999, and the Ph.D. degree in communication and information system from Jilin University, in 2003, where she is currently a Professor. She was a Postdoctoral Researcher with the Digital Media Institute, Tampere University of Technology, Finland, in 2003. From 2008 to 2008, she was a Visiting Professor with the Vienna University of Technology. From 2013 to 2014, she was a Visiting Professor with the University of Ottawa in Canada. Her research interests include image and video processing, multimedia signal processing, and error concealment for audio and video transmitted over unreliable networks.